Track variability of South China Sea-formed tropical cyclones modulated by seasonal and intraseasonal circulations

Jau-Ming Chen[1, *], Po-Hsiung Lin[2], Ching-Hsuan Wu[2], and Chung-Hsiung Sui[2]

[1] *Department of Maritime Information and Technology, National Kaohsiung University of Science and Technology, Kaohsiung City, Taiwan*
[2] *Department of Atmospheric Science, National Taiwan University, Taipei City, Taiwan*

ABSTRACT

Tracks of tropical cyclones (TCs) forming in the South China Sea (SCS) are examined in terms of their seasonal variability and associated modulations by seasonal and intraseasonal circulations. Three major TC tracks appear in the SCS: northeastward (NE) toward the Philippines and Taiwan, northward (N) toward southern China, and westward-northwestward (W-NW) toward the Indochina Peninsula and southwestern China. Seasonally, the dominant tracks are NE in May, from NE into W-NW in June, W-NW and N in July to September (JAS), and W-NW in October to November (ON). Formation of TCs with W-NW tracks is associated with a southeastward-extending monsoon trough (MT) and a northwestward-expanding western Pacific subtropical high (WPSH) in May to June (MJ), a southward-intensified MT and a westward-strengthened WPSH in JAS, and a northward and westward enhanced equatorial trough in ON. Formation of TCs with NE tracks in MJ is related to an eastward-intensified MT and an eastward-retreated WPSH. For TCs with N tracks, their formation is associated with an eastward and northward intensification of the MT and a northwestward extension of the WPSH. In terms of modulations of intraseasonal oscillations (ISOs), the 10-24-day and 30-60-day ISOs exert different effects on TC movement. For all track types, TCs tend to follow the propagation of the 10-24-day cyclonic anomaly and move along different tracks. The above movement comes under the influence of favorable environments in terms of moisture convergence provided by 30-60-day cyclonic anomalies distributing along TC tracks. The 10-24-day and 30-60-day ISOs exhibit comparable intensity to jointly modulate TC activity in the SCS.

1. INTRODUCTION

A tropical cyclone (TC) appearing in the South China Sea (SCS) can be formed locally in the SCS (108 - 120°E, 5 - 22°N) or remotely in the western North Pacific (WNP; 120 -180°E, 0 - 40°N) (Ling et al. 2016). In this study, the former TCs are referred to as SCS-formed TCs, while the latter TCs are migratory TCs (Chen et al. 2019). Climatologically, there are 10.5 TCs to appear in the SCS annually. Among them, 3.5 - 3.9 TCs are SCS-formed (Wang et al. 2007; Lin and Lee 2011). During the active TC season from July to November, the numbers of SCS-formed and migratory TCs are quite evenly distributed, reflecting the similar importance of these two types of TCs in affecting the SCS (Chen et al. 2017).

There are, however, clear seasonal, intraseasonal, and interannual variations in both SCS-formed and migratory TCs. For migratory TCs formed in the WNP, their interannual variability is closely regulated by El Niño-Southern Oscillation (ENSO). In an El Niño year, TC genesis tends to shift eastward/southeastward in accordance with an eastward extension of the monsoon trough (MT) and an eastward withdrawal of the western Pacific subtropical high (WPSH) (Lander 1994; Chen et al. 1998; Chia and Ropelewski 2002; Camargo et al. 2007; Zhan et al. 2011; Wu et al. 2012; Bell et al. 2014). Consequently, weakened easterly trade winds slow down the westward movement of TCs, leading to more

---

TCs recurving northward (Nakazawa and Rajendran 2007; Chen et al. 2009; Kim et al. 2012, 2013; Colbert et al. 2015). In a La Niña year, the MT is constrained in the western portions of the WNP and enhances TC genesis over there (Wang and Chan 2002; Chung and Li 2015). These formed TCs are spatially close to the SCS and thus have a better chance of entering the SCS (Chen et al. 2017). During 1960 - 2010, the averages of WNP TCs entering the SCS during fall are 1.53 in El Niño years and 3.64 in La Niña years (Tan et al. 2019). Similar processes also result in more WNP TCs making landfall in the Philippines in La Niña years than in El Niño years (Kubota and Chan 2009; Corporal-Lodangco et al. 2016).

On a shorter than interannual timescale, intraseasonal oscillations (ISOs) have been found to effectively modulate TC movement from the WNP into the SCS. The major subcomponents of ISOs are 10-24-day and 30-60-day modes (Hartmann et al. 1992; Chen and Chen 1995; Chen et al. 2000; Mao and Chan 2005; Ding 2007). In the WNP, convective ISO anomalies in the tropical region facilitate the westward/northwestward TC movement toward the SCS/ East Asia along the northern section of an anomalous cyclone (Li and Zhou 2013). In general, TCs tends to move with the propagating 10-24-day cyclonic anomaly under favorable background conditions from elongated 30-60-day cyclonic anomalies (Liebmann et al. 1994; Chen et al. 2018a). Chen et al. (2019) showed that ISO modulations on TC movement are associated with variability in seasonal background circulations of the MT and WPSH. TC movement from the WNP into the SCS is mainly steered by anomalous easterly flows. In July and August, the anomalous easterly flows locate in the southern periphery of a 30-60-day anticyclonic circulation in association with an enhanced WPSH. In September, 30-60-day anomalies steer TCs westward via anomalous easterly flows between an anomalous northern anticyclonic circulation and an anomalous southern cyclonic circulation. This circulation pair relates to a southeastward extension of the MT. In October and November, the anomalous easterly flows appear in the northern periphery of a 30-60-day cyclonic circulation resulting from an intensification of the equatorial trough.

The percentage of WNP TCs entering the SCS is lower in August-September and higher in June to July and October to November (Chen et al. 2017). This seasonal variability is determined by the location of TC genesis. TC genesis in August and September tends to be more northerly in accordance with the northward displacement of the MT and WPSH (Ding 1994; Lander 1996; Wu 2002; Su and Xue 2011). As such, TCs tend to move northward towards the northern North Pacific or northwestward toward East Asia, reducing the possibility of movement toward the SCS.

For SCS-formed TCs, ENSO influences interannual variability in genesis number. El Niño years feature warm sea surface temperature (SST) anomalies in the tropical east-

ern Pacific which in turn induce a downward branch to tropical Walker circulations and an anomalous divergent center over the Maritime Continent (Wang 1992; Klein et al. 1999; Lau and Nath 2000, 2003). Northwest of this anomalous divergence center, an anomalous anticyclonic circulation appears in the SCS suppressing TC formation during fall (Chen 2011). By contrast, La Niña years tend to enhance TC formation in the SCS during fall (Chan 2000). Seasonally, Wang et al. (2007) showed that SCS-formed TCs occur mainly in the northern basin during May to September, and in the southern basin during October to December. The former is facilitated by enhanced low-level vorticity and weakened vertical wind shear, while the latter is assisted by better thermal and dynamic environments in the southern basin than the northern basin during the cold season.

ISO influence on TC genesis in the SCS exhibits systematic characteristics. In general, ISOs enhance (suppress) TC formation during their active (inactive) phase (Hall et al. 2001; Barrett and Leslie 2009; Chand and Walsh 2010; Klotzbach 2014). Enhanced TC formation is mainly caused by strong cyclonic anomalies extending from the SCS to the WNP (Chen et al. 2018b). In May to June, a northward propagating ISO across the SCS can modulate TC genesis in the SCS (Huang et al. 2011). In terms of TC movement, TCs formed in the SCS during summer tend to be steered westward along the southern section of weakened ISO convection in the northern SCS in relation to a westward-intensified WPSH (Ling et al. 2016). During June to October, the eastward propagating ISOs tend to steer one third of SCS-formed TCs eastward, while the other two thirds of SCS-formed TCs are steered by seasonal easterly flows westward (Yang et al. 2015).

The above literature review indicates that past research regarding ISO influence on movement of SCS-formed TCs mainly focuses on two tracks, either eastward or westward. However, SCS-formed TCs exhibit other track types. Figure 1a shows tracks of all SCS-formed TCs (delineated by Joint Typhoon Warning Center best track data) with formation times in May to November for the period 1979 - 2010. TC movement can be categorized into three major tracks (Fig. 1b): northeastward (NE) toward the Philippines and Taiwan, northward (N) toward southern China, and westward-northwestward (W-NW) toward southwestern China and the Indochina peninsula. Variability features of TCs with these three track types throughout the entire TC season and associated modulatory processes by seasonal and ISO circulations have not been comprehensively compared and examined. This study examines the following questions to gain greater insight into track variability of SCS-formed TCs:

(1) Is there any noticeable seasonal variability in tracks of SCS-formed TCs? If yes, how do seasonal background circulations of the MT and WPSH affect the variability of TC tracks?

(2) How do ISOs modulate movement of SCS-formed TCs? What are the relative roles of 10-24-day and 30-60-day ISOs in the modulating processes?

The examinations of these questions should help us better understand the modulating processes imposed by seasonal and intraseasonal circulations on TC activity in the SCS. These analysis results may provide guidance in monitoring of variability features pertaining to key large-scale circulations, having the potential to improve TC forecasts.

2. DATA

The large-scale patterns of seasonal and ISO circulations are illustrated by the European Center for Medium-Range Weather Forecasts (ECMWF) ERA-interim reanalysis data (e.g., Dee et al. 2011). The ERA-interim data have a global domain with a spatial resolution on a 0.75° longitude × 0.75° latitude grid. The fields of wind, streamfunction, and geopotential height are used to depict variability patterns of large-scale circulations and steering flows associated with TC movement. TC activity is depicted by the 6-hr best track data obtained from the Joint Typhoon Warning Center (JTWC). The JTWC data offer information on genesis locations, movement tracks, and genesis number for SCS-formed TCs. Outgoing longwave radiation (OLR) data are obtained from National Oceanic and Atmospheric Administration (NOAA). They are daily data and used to illustrate convection variability associated with ISOs. Their resolution is on a 2.5° longitude × 2.5° latitude grid for the entire globe (Liebmann and Smith 1996). The analysis period of this study is from 1979 to 2010.

3. SEASONAL VARIABILITY IN TRACKS OF SCS-FORMED TCS

TCs with formation inside the SCS domain (108 - 120°E, 5 - 22°N) are defined as SCS-formed TCs in this study. 1979 - 2010 accumulated numbers of SCS-formed TCs for each calendar month are shown in Fig. 2. TC formation in the SCS is active during May to November with a number greater than 10 and inactive in the remaining months with a number less than 3. SCS-formed TCs are maximum in number in September and do not form in February and March. Analysis of TC tracks thus focuses on the active TC season of May to November that has 132 TCs, about 95% of a total of 139 SCS-formed TCs during 1979 - 2010.

As shown in Fig. 1, major tracks of SCS-formed TCs can be separated into three types: northeastward (NE) toward the Philippines and Taiwan, northward (N) toward southern China, and westward-northwestward (W-NW) toward the Indochina Peninsula and southwestern China. TCs with an irregular track that do not fit into the above three track types are categorized as the other type (OTHER). The climatological distributions of SCS-formed TCs with

different track types from May to November are shown in Table 1. SCS-formed TCs in May primarily exhibit a NE track (10 TCs). In June, TC tracks tend to switch from NE (4 TCs) into W-NW (9 TCs). From July to September, TCs with W-NW tracks dominate (10 - 22 TCs), which are followed by TCs with N tracks (4 - 6 TCs). In October to November, most TCs take W-NW tracks (12 - 19 TCs). In the active TC season from May to November, W-NW tracks have the largest number (86 TCs), followed by NE (22 TCs), N (17 TCs), and OTHER (7 TCs) tracks.

4. CIRCULATIONS ASSOCIATED WITH SEASONAL VARIABILITY OF TC TRACKS

Table 1 reveals the existence of seasonal variability in tracks of SCS-formed TCs. How do large-scale circulations surrounding the SCS connect with this seasonal track variability? Seasonal variability of TC tracks characterizes an apparent change from dominant NE tracks in May into primary W-NW tracks in July to November. The transition occurs in June from NE tracks to W-NW tracks. In June, three out of four TCs with NE tracks form before 10 June. Among them, the latest one forms on 10 June and vanishes on 13 June. On the other hand, seven out of nine TCs with W-NW tracks form after 16 June. This indicates that major TC tracks are NE before 15 June and W-NW after 16 June which is consistent with dominant track features in May and July, respectively. On average, the life spans of TCs occurring in the periods of May, 1 - 15 June, and 16 - 30 June are 3.3, 3.7, and 2.4 days, respectively. This indicates that SCS-formed TCs with major NE tracks in May and early June tend to live longer than TCs with major W-NW tracks in late June.

The large-scale circulations associated with TC track variability are illustrated by composite patterns of total (real-time) 850-hPa streamfunction (S850) and steering flows integrated from 850 to 300 hPa for TCs forming in different seasonal periods. These composite patterns are averaged from the formation day and ensuing two days. Transitional features of TC tracks in June are illustrated by composite patterns for TCs forming in the periods of 1 - 15 June and 16 - 30 June in Fig. 3. Also included is the difference in these two composite patterns (16 - 30 June minus 1 - 15 June). Formative locations of TCs are superimposed on the circulation patterns. TC formation in early June (Fig. 3a) mainly occurs on the eastern and southern peripheries of a deepened trough extending from southern China eastward into the SCS. These TCs are later able to follow southwesterly flows to take a NE track toward the Philippines and Taiwan. In late June (Fig. 3b), SCS-formed TCs have their genesis inside a southeastward intense trough extending from southern China into the SCS. The southeasterly flows on the eastern section of this deepened trough act to steer TCs with a W-NW track. The difference patterns shown in Fig. 3c disclose changes
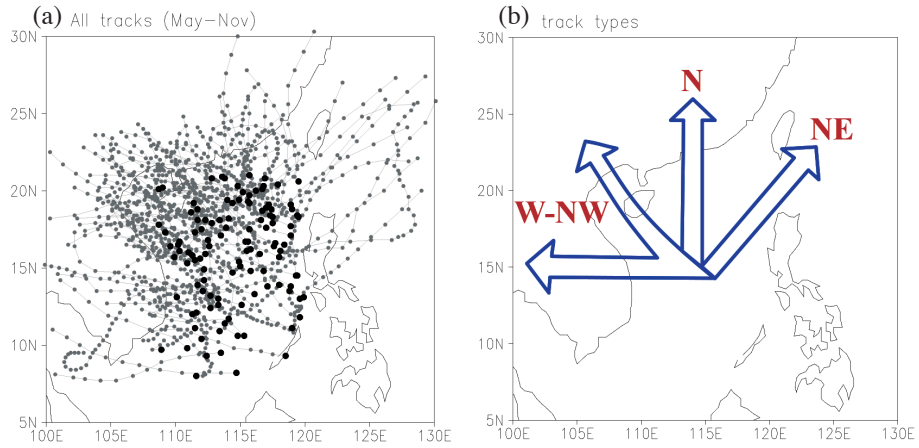
Fig. 1. (a) Track distributions of TCs forming in the South China Sea (108 - 120°E, 5 - 22°N) in the May to November season during 1979 - 2010. (b) Schematic diagrams of major TC tracks in the SCS: northeastward (NE) toward the Philippines-Taiwan region, northward (N) toward southern China, and westward-northwestward (W-NW) toward the Indochina Peninsula and southwestern China.
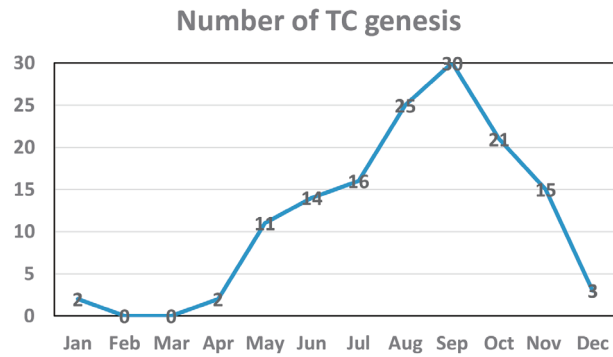

Fig. 2. Climatological monthly numbers of TCs forming inside the SCS accumulated from 1979 to 2010.

Table 1. Climatologically numbers of TC formation in the SCS with different tracks from May to November accumulated from the period 1979 - 2010. The tracks are northeastward (NE), westward-northwestward (W-NW), northward (N), and the other type (OTHER).

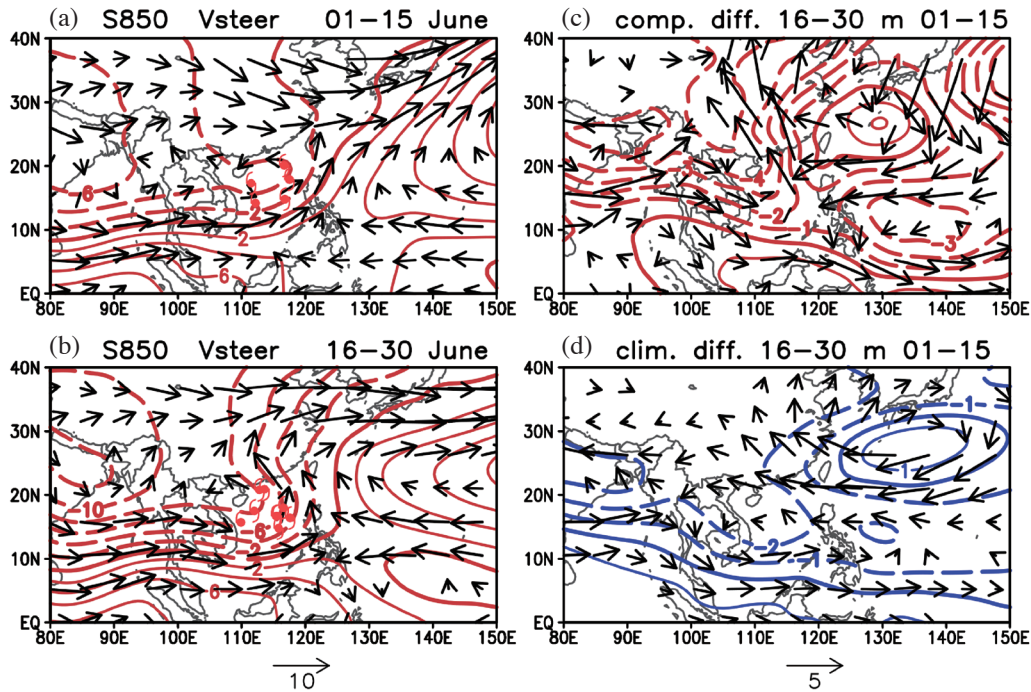|	NE	W-NW	N	OTHER
May	*10*	1	0	0
June	*4*	*9*	1	0
July	2	*10*	*4*	0
August	2	*13*	*6*	4
September	2	*22*	*5*	1
October	0	*19*	1	1
November	2	*12*	0	1
total	22	86	17	7

Fig. 3. Composite patterns of 850-hPa streamfunction (S850) and steering flows integrated from 850 to 300 hPa associated with SCS-formed TCs forming in the periods of (a) 1 - 15 June and (b) 16 - 30 June. The difference in these two composite patterns [(b) minus (a)] is shown in (c). The corresponding difference in climatological circulations (16 - 30 June minus 1 - 15 June) is shown in (d). In (a) and (b), the composite patterns are averaged from the formation day and ensuing two days and the formative locations of TCs are marked by TC symbols. Contour intervals are 2×10^6 m^2 s^{-1} in (a) and (b) and 1×10^5 m^2 s^{-1} in (c) and (d).

in TC tracks from NE into W-NW in late June being facilitated by a southeastward deepened MT over the SCS and an intense WPSH to the northeast of the SCS. The above large-scale circulation changes may relate to variability in background seasonal circulations. The difference in climatological circulations between the periods of 1 - 15 June and 16 - 30 June (latter minus former) is shown in Fig. 3d. The climatological difference patterns resemble the difference patterns in Fig. 3c by exhibiting a deepened trough over the SCS and an intensified subtropical high on its northeastern side. However, the deepened tough over the SCS is much stronger in Fig. 3c than Fig. 3d. The climatological circulation may partially provide a favorable background for TC track transition in June, but is not strong enough to control this variability. There is a need for sub-seasonal disturbances to cause TC track changes.

Another interesting seasonal feature is a change from W-NW and N tracks in July to September (JAS) to a dominant W-NW track in October to November (ON). To investigate this seasonal variability feature, composite patterns of circulations and steering flows associated with SCS-formed TCs in JAS and ON are examined via the composite patterns from the formation day and ensuing two days. As shown in Fig. 4a, genesis of SCS-formed TCs in JAS is embedded in a zonally elongated trough with its center over the northern SCS north of 15°N. TCs are guided by cyclonic steering

flows to take a W-NW or N track. In ON (Fig. 4b), SCS-formed TCs tend to gather within a cyclonic center over the southern SCS south of 15°N, while a zonally-elongated subtropical high exists to the north of the SCS. TCs forming in the southern SCS are constrained by the zonally-extended subtropical high on their northern side and thus follow southeasterly and easterly steering flows in the northern SCS to move with a W-NW track. The difference between composite patterns of JAS and ON (JAS minus ON) in Fig. 4c exhibits a cyclonic circulation covering China and the northern SCS and an anticyclonic circulation in the southern SCS. The corresponding difference patterns of the climatological circulations between JAS and ON (Fig. 4d) resemble the difference patterns in Fig. 4c. These two difference patterns have comparable magnitudes. This suggests that track variability between JAS and ON is closely related to the seasonal march of background seasonal circulations.

5. CIRCULATION FEATURES FOR TC FORMATION WITH DIFFERENT TRACKS

In addition to seasonal variability in TC tracks, it is also of interest to examine circulation features associated with TC formation for different track types. Other than vertical-integrated flows, the environmental steering flows can be simply represented by 500-hPa winds (Chan 2000;
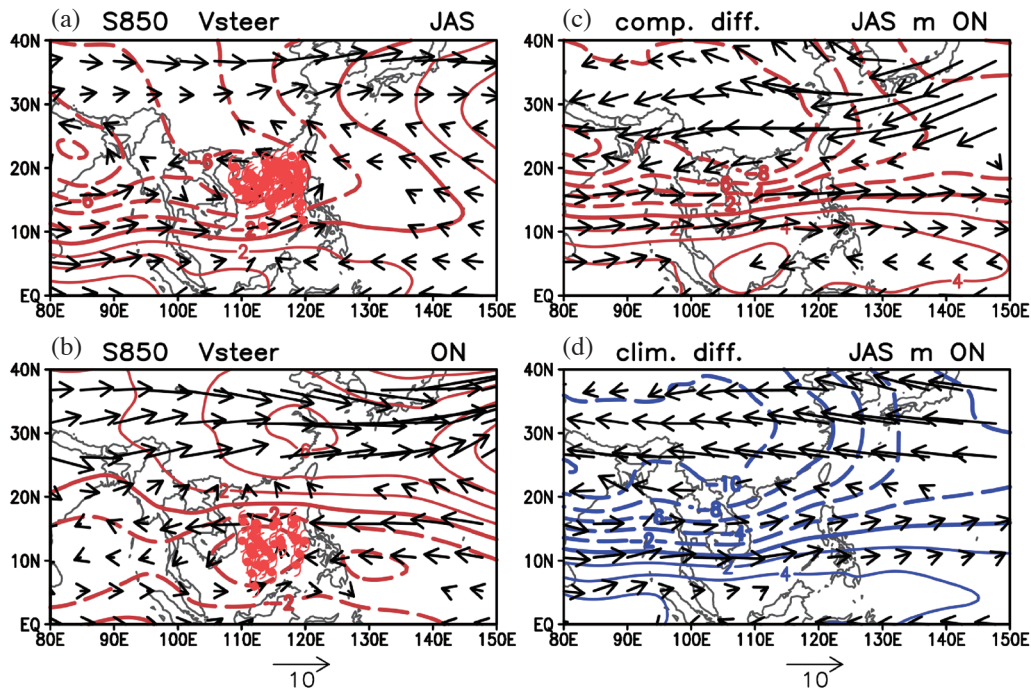
Fig. 4. As in Fig. 3, except for composite patterns of S850 and steering flows for SCS-formed TCs forming in the periods of (a) July to September (JAS) and (b) October to November (ON). The difference patterns (JAS minus ON) of composite circulations and climatological circulations are shown in (c) and (d), respectively. Contour intervals are 2×10^6 m^2 s^{-1}.

Tu and Chen 2019). The composite streamline patterns of 500-hPa winds (V500) on TC formation days for different track types are illustrated in Fig. 5. Composite circulations for TCs with W-NW tracks in May to June (MJ), JAS, and ON are compared with those with NE tracks in MJ and N tracks in JAS.

For TCs with W-NW tracks, the total streamline pattern on their formation days exhibits a similar feature in MJ (Fig. 5a), JAS (Fig. 5b), and ON (Fig. 5c). TCs tend to form within a cyclonic circulation overlying the SCS that is adjacent to an extended anticyclonic circulation on the northern side. The cyclonic and anticyclonic circulations reflect the spatial distribution of the existing MT (or equatorial trough) and WPSH. The easterly flows between the cyclonic and anticyclonic circulations extend westward across the SCS to reach the Indochina Peninsula. These easterly flows steer TCs to take a W-NW track. Meanwhile, the WPSH to the north of the SCS blocks the chance of TCs from moving northward. Average locations of formation for all TCs with W-NW tracks are 114.1°E, 16.6°N in MJ, 114.6°E, 17.4°N in JAS, and 114.2°E, 12.6°N in ON. The major difference in formative locations appears to be the JAS having a more northerly location (17.4°N) and ON a more southerly location (12.6°N). This follows well the meridional displacement of the MT and WPSH.

The composite circulations on formation days of TCs with NE tracks in MJ (Fig. 5d) and with N tracks in JAS (Fig. 5e) also contain some common features. TCs for these two types tend to form in a cyclonic shear/circulation over the SCS with a relatively lower pressure region on the northern side. Their differences appear in the flow patterns of this cyclonic shear. For NE tracks, the cyclonic shear is adjacent to an anticyclonic circulation to the east. TCs tend to form in the eastern half of the SCS. After formation, the strong southerly flows between the cyclonic and anticyclonic circulations over the eastern SCS effectively drive TCs northward at first. On the northern side north of 25°N, the prevailing westerly flows provide an environment assisting TC movement eastward, resulting in NE tracks. There are three TCs that formed in the southwestern SCS. They followed the westerly flows of the cyclonic shear eastward into the eastern SCS and then caught southerly flows to move northward and later eastward. TCs with N tracks in JAS form within a cyclonic circulation. After TC formation in the SCS, the southeasterly flows in the eastern SCS can drive TCs northward toward a relatively lower pressure region in southern China. The prevailing westerly flows displace northward to the north of 35°N giving room for TCs to move northward into southern China before moving eastward. As such, TCs of this type take a northward track from the northern SCS to make landfall in southern China. The average locations for formation are 115.8°N, 15.1°N for TCs with NE tracks in MJ and 114.9°N, 19.0°N for TCs with N tracks in JAS. TCs with NE tracks tend to form in a more easterly region (115.8°N) and are thus easily driven by southwesterly flows at the western boundary of the WPSH to move northeastward.
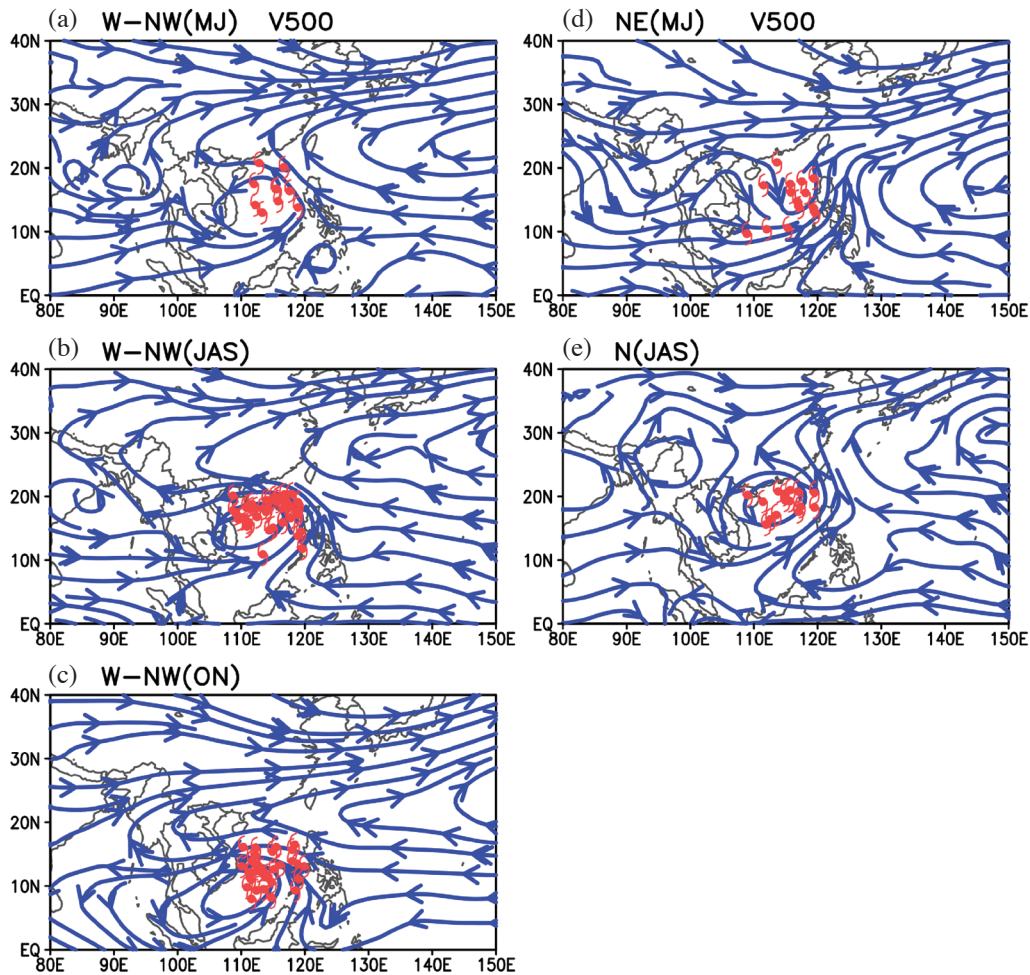
Fig. 5. Composite streamline patterns of 500-hPa winds on the formation day of TCs for different tracks in different seasonal periods: (a) W-NW tracks during May to June, (b) W-NW tracks during July to September, (c) W-NW track during October to November, (d) NE tracks during May to June, and (e) N tracks during July to September. TC locations on the formation day in each period are marked by TC symbols.

TCs with N tracks tend to form in a more northerly region (19.0°N) than TCs of other track types. These TCs are closer to southern China and thus have a better chance of moving northward and making landfall there.

The large-scale circulation patterns of the MT and WPSH have been found to exert evident influence over TC formation and consequent movement (Harr and Elsberry 1991; Nakazawa and Rajendran 2007; Chen et al. 2009, 2019; Ko and Hsu 2009). Their variability features can be applied to the monitoring and prediction of TC activity. To jointly demonstrate variability of the MT and WPSH associated with different TC tracks, 850-hPa geopotential height (Z850) is composited for the formation days of TCs with different track types (Fig. 6). Vertically-integrated steering flows are superimposed on Z850 to delineate steering effects over TC movement. The 1480-, 1490-, and 1500-gpm Z850 contours are used to show composite variability features (red contours). By making comparisons with the climatological mean (blue contours), formation of TCs with W-NW tracks can be seen to be facilitated by a southeastward-extending MT in MJ (Fig. 6a), by a southward-intensified MT in JAS (Fig. 6b), and by a northward and westward enhanced equatorial trough in ON (Fig. 6c). The steering flows reveal that the southeasterly flows in the eastern SCS and the easterly flows in the northern SCS are responsible for steering TCs to take a W-NW track. These easterly flows in the northern SCS are associated with a moderate northwestward intensification of the WPSH in MJ, by a strong westward intensification of the WPSH in JAS, or by a strong northward intensification of the equatorial trough in ON.

For formation of TCs with NE tracks in MJ, the salient features are an eastward intensification of the MT and an eastward retreat of the WPSH (Fig. 6d). In contrast with the W-NW tracks of Fig. 6a, the eastward-shifted WPSH causes the disappearance of easterly flows to the north of the SCS. Instead, the westerly steering flows appear to facilitate eastward TC movement. As such, TCs are steered to move northward and later eastward resulting in a NE track.
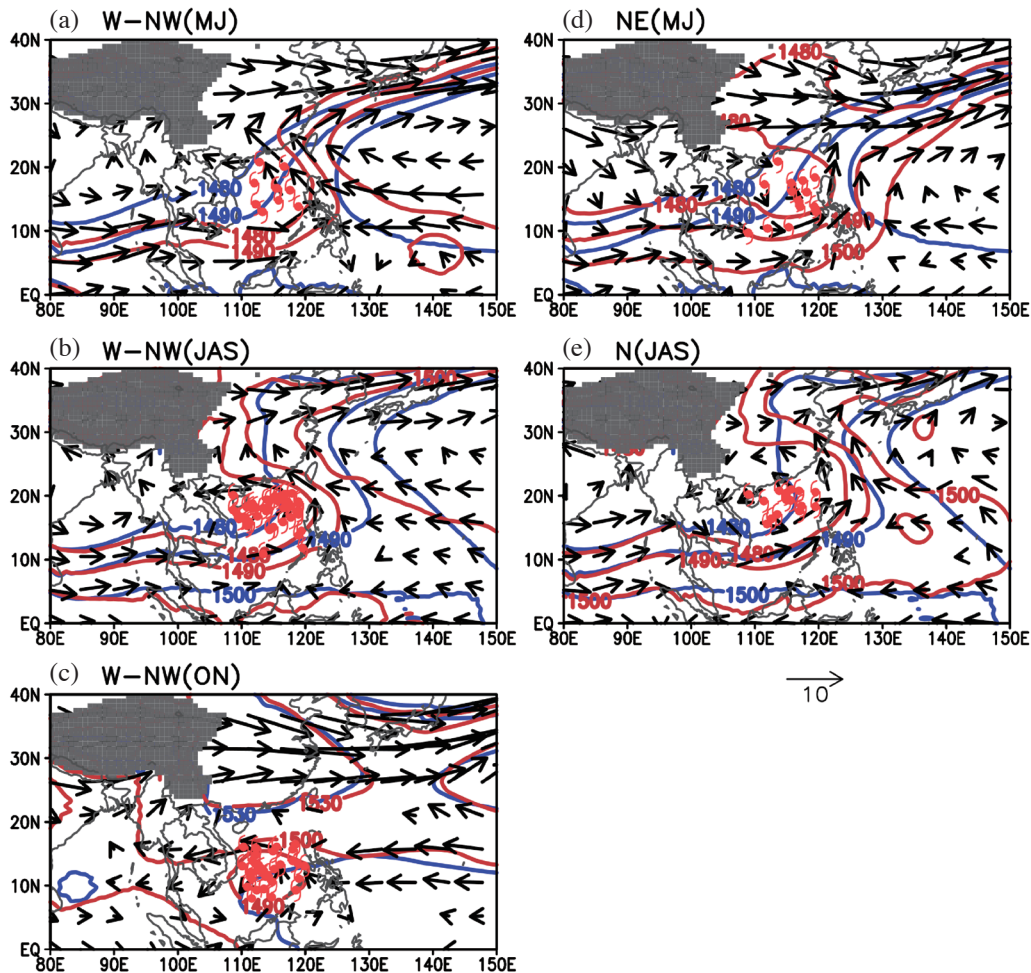
Fig. 6. As in Fig. 5, except for composite patterns of 850-hPa geopotential height and steering flows integrated from 850 to 300 hPa on the formation day of TCs for different tracks in different seasonal periods. Climatological mean circulations are illustrated by blue contours, while composite circulations for TC formation days are represented by red contours.

Formation of TCs with N tracks (Fig. 6e) is associated with a strong eastward and northward intensification of the MT and a northwestward expansion of the WPSH. The MT has a stronger intensification toward the north in N tracks than in W-NW tracks. The composite 1490-gpm contour around 120°E is located at around 23°N in W-NW tracks, but farther north at around 30°N in N tracks. This great northward expansion of the MT provides southerly steering flows in the central and eastern SCS to guide TCs moving northward into a lower-pressure region over southern China for development, resulting in northward tracking TCs.

6. ISO MODULATIONS ON W-NW-TRACK TCS

Chen et al. (2018a) and Tan et al. (2019) found that TC activity is under the systematic modulation of ISOs. The modulatory effects of 10-24-day and 30-60-day ISOs on TC movement in W-NW tracks are examined in this section. The day of TC formation is defined as day 0, while N days thereafter is defined as day N. Composite patterns of 10-24-day and 30-60-day S850 anomalies associated with TCs with W-NW tracks in MJ, JAS, and ON from day 0 to day 2 and day 4 are exhibited in Figs. 7, 8, and 9, respectively. Hereafter, composite S850 anomalies significant at the 0.1 level of the Student-*t* test are shaded. Superimposed on S850 anomalies are corresponding 10-24-day or 30-60-day anomalies of steering flows vertically integrated from 850 to 300 hPa. Actual TC tracks with a TC symbol to mark the genesis location are superimposed on day-0 circulation anomalies. The 10-24-day and 30-60-day anomalies of S850 and steering flows are extracted by a Lanczos bandpass filter scheme (Duchon 1979). In MJ, TCs with W-NW tracks tend to form around the center of a significant 10-24-day cyclonic anomaly that extends from the SCS westward (Fig. 7a). TCs follow the northwestward propagation of this cyclonic anomaly to move toward southwestern China and the Indochina Peninsula from day 2 to day 4 (Figs. 7b - c). For the 30-60-day ISO, TC formation occurs around a regional center of the 30-60-day cyclonic anomaly over the SCS (Fig. 7d). The W-NW movement of TCs from day 2 to
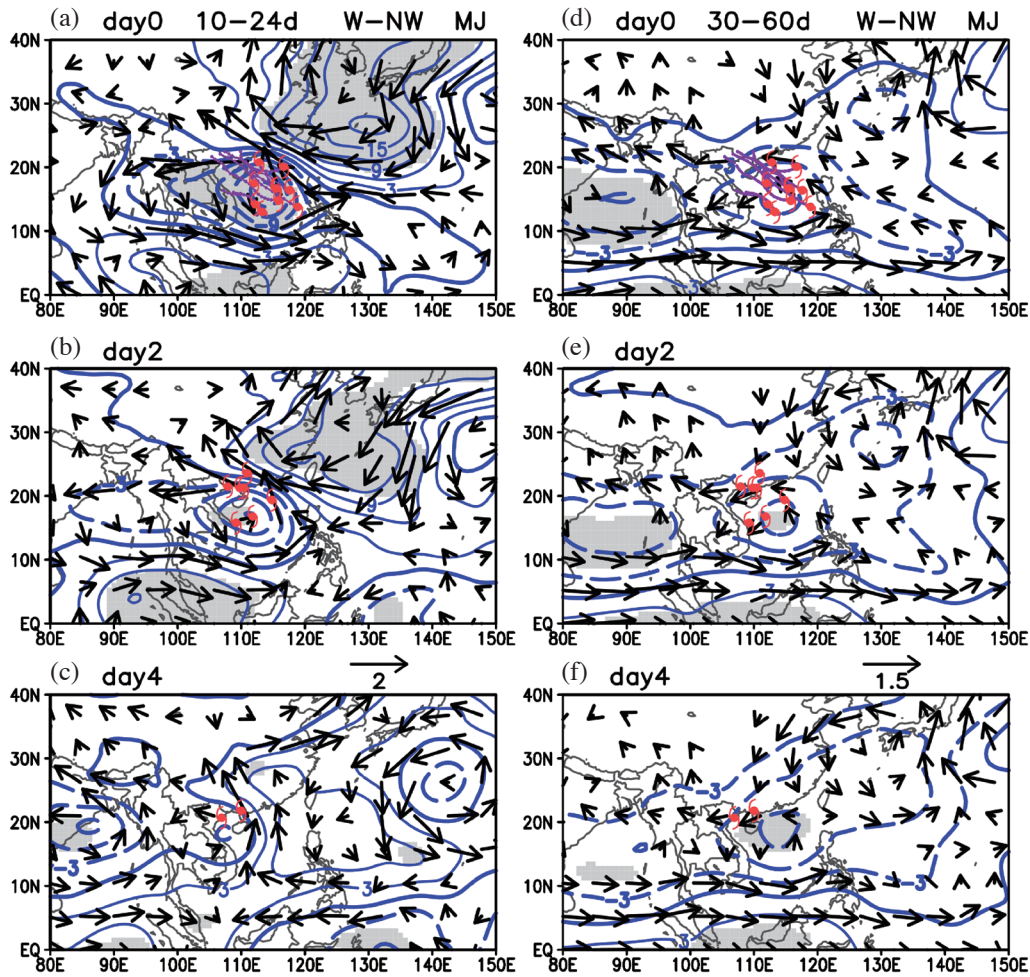
Fig. 7. Composite patterns of 10-24-day/30-60-day S850 anomalies for TCs with W-NW tracks during May to June for different evolutionary phases: (a)/(c) day 0, (b)/(d) day 2, and (c)/(f) day 4. Corresponding 10-24-day and 30-60-day anomalies of steering flow (vertically integrated from 850 to 300 hPa) and actual TC tracks are superimposed on day 0. Locations of TCs in each phase are marked by TC symbols. Contours are 3×10^5 m^2 s^{-1}. Composite anomalies significant at the 0.1 level of the Student-t test are shaded.
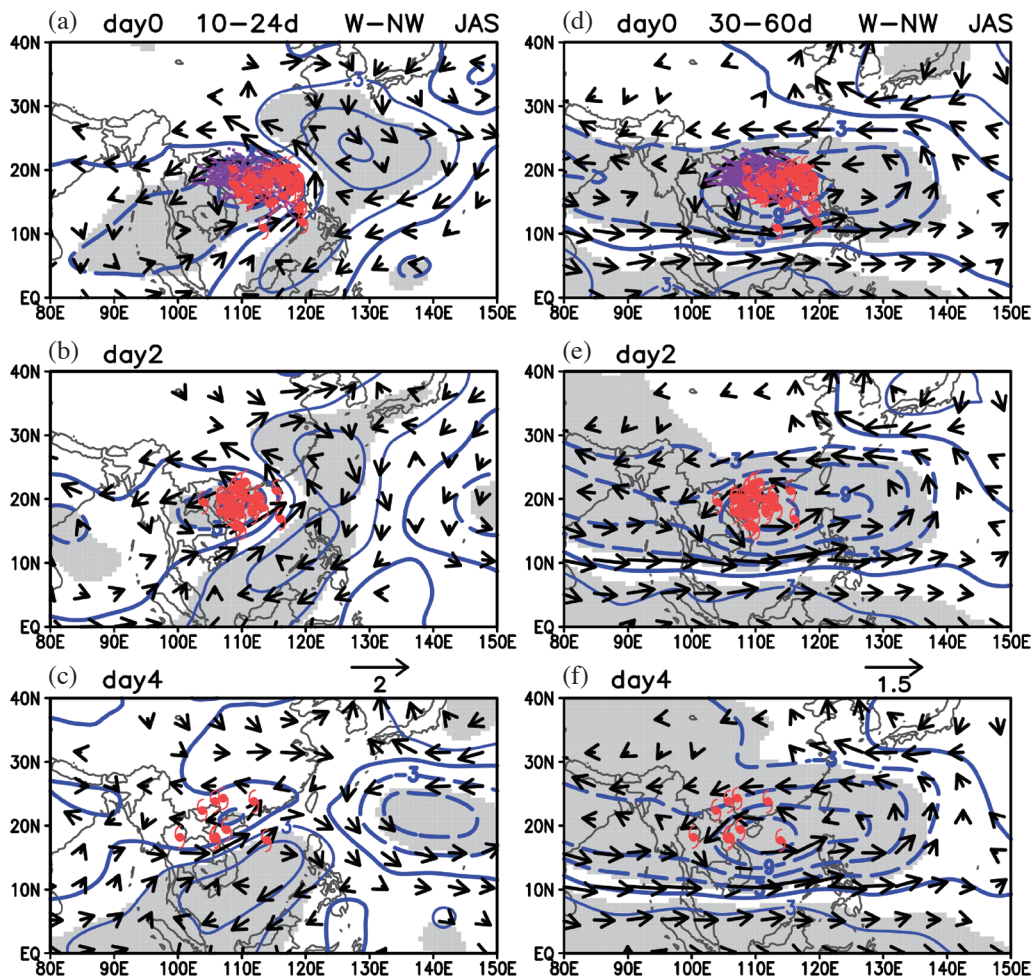
Fig. 8. As in Fig. 7, except for composite patterns of 10-24-day/30-60-day S850 and steering flow anomalies for TCs with W-NW tracks during July to September: (a)/(c) day 0, (b)/(d) day 2, and (c)/(f) day 4.
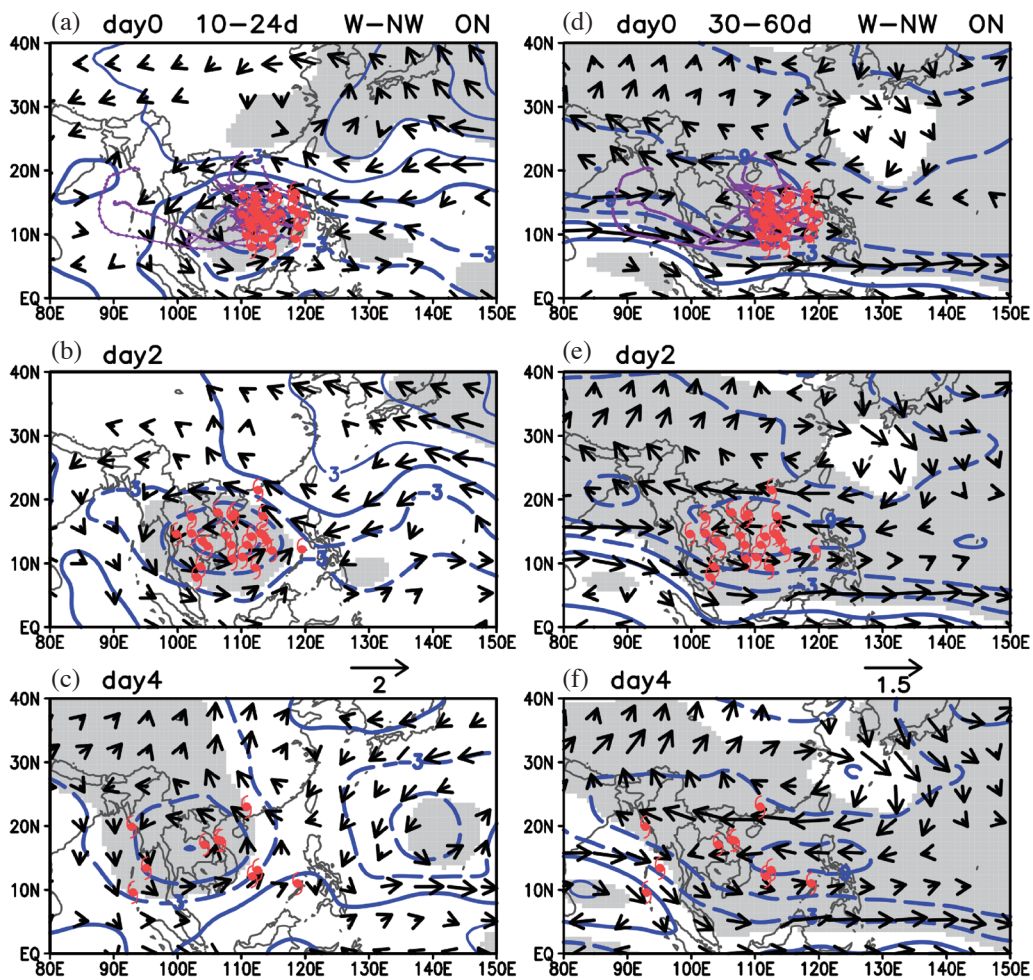
Fig. 9. As in Fig. 7, except for composite patterns of 10-24-day/30-60-day S850 and steering flow anomalies for TCs with W-NW tracks during October to November: (a)/(c) day 0, (b)/(d) day 2, and (c)/(f) day 4.

day 4 tend to be driven by anomalous easterly and southeasterly steering flows in the eastern and northern sections of the elongated 30-60-day cyclonic anomaly (Figs. 7e - f). During TCs' W-NW movement, the 10-24-day cyclonic anomaly propagates northwestward leading to TC movement, while the 30-60-day cyclonic anomaly propagates northward slowly to supply the steady large-scale favorable conditions and steering flows for the development and movement of TCs.

In JAS, TCs with W-NW tracks mainly form inside the center of a significant 10-24-day cyclonic anomaly (Fig. 8a) and move along with the northwestward propagation of this cyclonic anomaly toward southwestern China on day 2 and day 4 (Figs. 8b - c). This W-NW TC movement is completely embedded in a zonally elongated and significant 30-60-day cyclonic anomaly (Figs. 8d - f). Such TC movement is mainly guided by anomalous easterly steering flows along the northern periphery of the 30-60-day cyclonic anomaly. The 30-60-day cyclonic anomaly has its center more-or-less stationary over the SCS to assist TC formation and provide persistent steering flows to guide ensuing TC movement.

In ON, TCs with W-NW tracks tend to form in a more southern region to the south of 18°N (Fig. 9a). These TCs gather around the center of a significant 10-24-day cyclonic anomaly on day 0 and mainly move toward the Indochina Peninsula along with the northwestward propagation of the 10-24-day cyclonic anomaly on day 2 and day 4 (Figs. 9b - c). Meanwhile, TC formation and movement from day 0 to day 4 result from the favorable environment supplied by a significant 30-60-day cyclonic anomaly (Figs. 9d - f). This anomaly extends from the northwest to the southeast from South Asia across the SCS into the tropical WNP. The paths of northwestward-moving TCs mainly follow the central region of the 30-60-day cyclonic anomaly. Anomalous easterly steering flows in the central and northern regions of the 30-60-day cyclonic anomaly act to facilitate westward and northwestward TC movement.

7. ISO MODULATIONS ON TCS WITH NE OR N TRACKS

The modulatory processes of ISOs on TCs with NE or N tracks are examined in this section. For TCs with NE tracks in MJ, TC formation inside the SCS is located around the center of a significant 10-24-day cyclonic anomaly with a northeastward extension into the northwestern Pacific (Fig. 10a). On day 2, the center of the 10-24-day cyclonic anomaly propagates northeastward toward Taiwan, while TCs follow the propagation of the cyclonic center to move northeastward (Fig. 10b). On day 4, the cyclonic center continuously moves northeastward to overlie Taiwan (Fig. 10c). TCs move faster than this cyclonic center to the region northeast of Taiwan placing them along the northeasterly extension of the 10-24-day cyclonic anomaly. The 30-60-day ISO also exhibits a significant cyclonic

center over the SCS during TC formation (Fig. 10d). This 30-60-day cyclonic anomaly extends from the SCS northeastward into the northwestern Pacific on day 2 and day 4 (Figs. 10e - f). Anomalous westerly and southwesterly flows in the southern and eastern sections of the 30-60-day cyclonic anomaly steer TCs northeastward toward the northwestern North Pacific. The 30-60-day cyclonic anomaly shows a slow northward propagation from day 0 to day 4.

For TCs with N tracks in JAS, the salient 10-24-day feature on day 0 is a significant cyclonic anomaly extending from the northern SCS northward into southern China (Fig. 11a). It moves northward overland with a rapidly decaying center on day 2 (Fig. 11b), which disappears completely on day 4 (Fig. 11c). TCs form inside the northern SCS within the 10-24-day cyclonic center on day 0 and follow its northward propagation to make landfall over southern China on day 2. All TCs die off on day 4, this being two days after making landfall. For the 30-60-day anomaly, it shows a significant and isolated center across the northern SCS and southern China facilitating TC formation on day 0 (Fig. 11d). This cyclonic center provides anomalous southerly flows in its eastern sections to guide SCS-formed TCs northward on day 2 (Fig. 11e). However, its intensity decays quickly on day 2 and almost vanishes on day 4 (Fig. 11f). The 30-60-day cyclonic center is more-or-less stationary.

To quantitatively measure the relative role of 10-24-day and 30-60-day ISOs in the modulation of TC movement, intensity of their associated convection anomalies is examined. Composite anomalies of 10-24-day and 30-60-day OLR for day 0 of TCs with N-NW tracks during MJ, JAS, and ON are shown in Fig. 12. Superimposed on OLR anomalies are the locations of TC genesis. Composite OLR anomalies significant at the 0.1 level of the Student-t test are shaded. Figure 12 illustrates that TCs tend to form around the central region of a convective (negative) anomaly of the 10-24-day ISO, but in a regional center of an elongated convective anomaly of the 30-60-day ISO. The spatial patterns of convective anomalies largely resemble cyclonic anomalies of S850 shown in Figs. 7, 8, and 9. For TCs with N tracks in MJ and NE tracks in JAS, their composite OLR anomalies for 10-24-day and 30-60-day ISOs on day 0 are shown in Fig. 13. For both 10-24-day and 30-60-day modes, TCs tend to gather around the centers of convective anomalies which provide favorable environments for TC formation. The intensity of 10-24-day and 30-60-day ISOs are measured for OLR anomalies averaged over the central SCS in the 110 - 120°E, 10 - 20°N region. As shown in Table 2, 10-24-day OLR has stronger intensity than 30-60-day OLR in most TC track types, except for a minor weakness in intensity in the NE track type during MJ. The intensity of 10-24-day OLR is much larger than that of 30-60-day OLR for TCs with W-NW tracks during MJ, and slightly stronger or comparable for TCs with W-NW and N tracks in JAS and W-NW tracks in ON. The analysis of ISO intensity
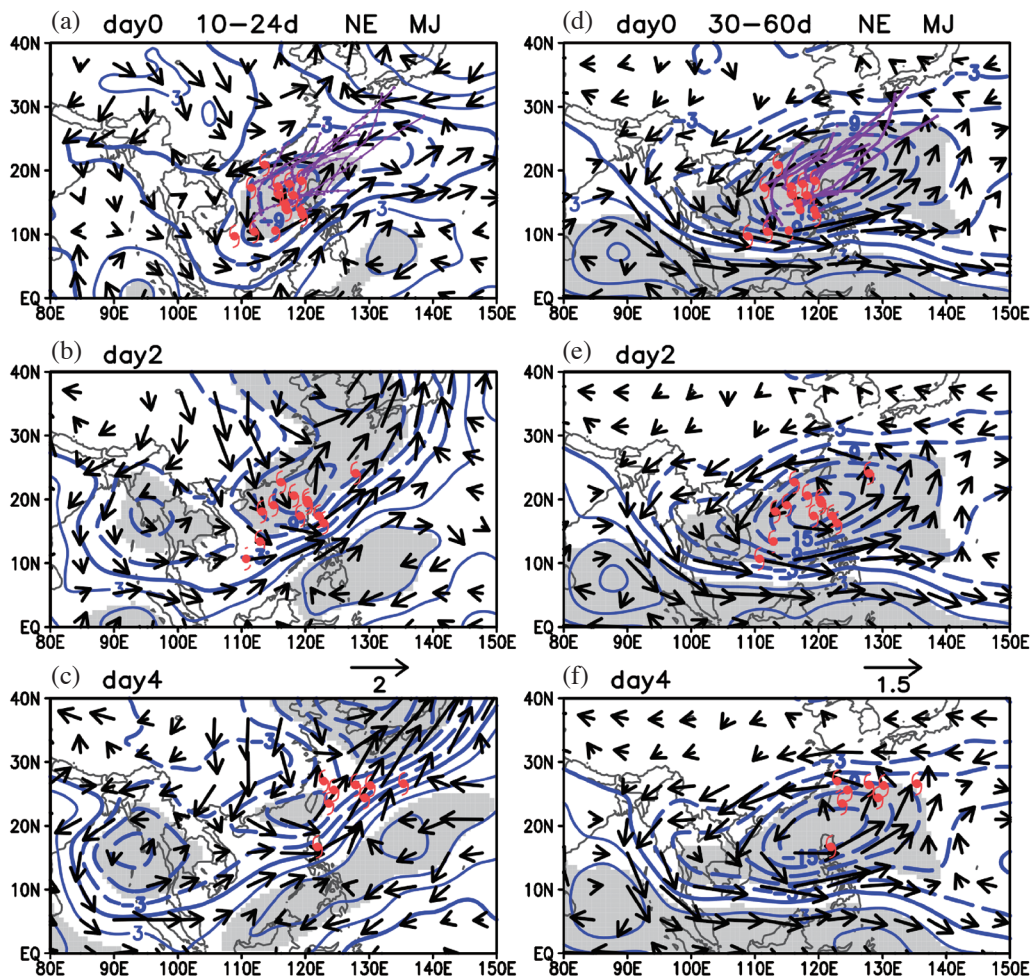
Fig. 10. As in Fig. 7, except for composite patterns of 10-24-day/30-60-day S850 and steering flow anomalies for TCs with NE tracks during May to June: (a)/(c) day 0, (b)/(d) day 2, and (c)/(f) day 4.
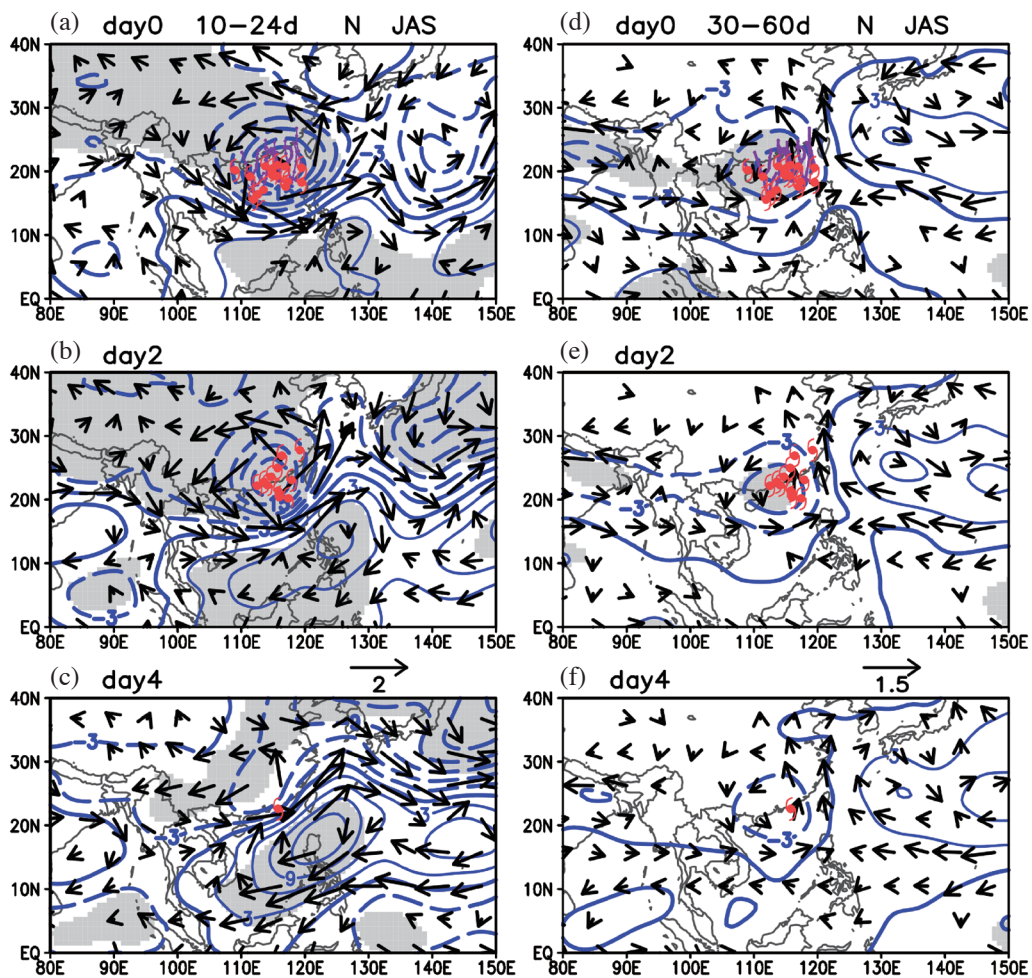
Fig. 11. As in Fig. 7, except for composite patterns of 10-24-day/30-60-day S850 and steering flow anomalies for TCs with N tracks during July to September: (a)/(c) day 0, (b)/(d) day 2, and (c)/(f) day 4.
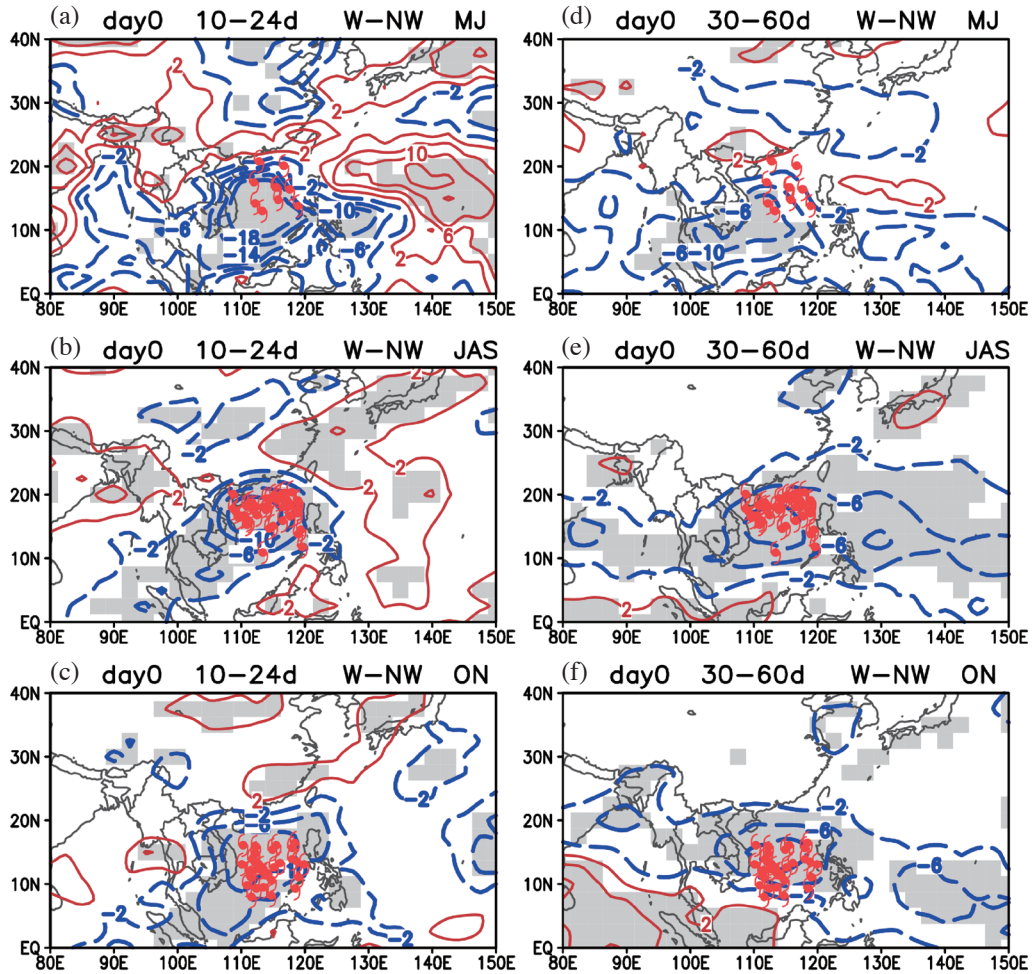
Fig. 12. Composite patterns of 10-24-day/30-60-day OLR anomalies for TCs with W-NW tracks during (a)/(d) May to June, (b)/(e) July to September, and (c)/(f) October to November. OLR anomalies significant at the 0.1 level of the Student-t test are shaded. TC genesis locations are marked by TC symbols. Contour intervals of OLR anomalies are 4 W m^{-2}.
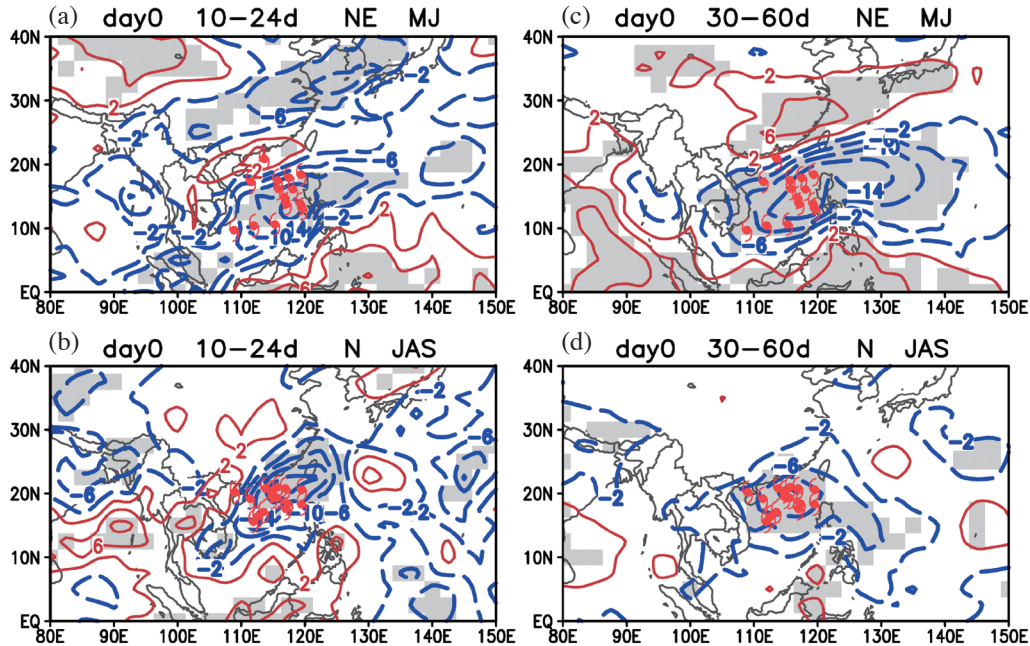
Fig. 13. As in Fig. 12, except for composite patterns of 10-24-day/30-60-day OLR anomalies for (a)/(c) TCs with NE tracks during May to June and (b)/(d) TCs with N tracks during July to September.

Table 2. Values of 10-24-day and 30-60-day OLR anomalies averaged over the central SCS in the 110 - 120°E, 10 - 20°N region for day 0 of different TC track types in different seasonal periods (unit: W m⁻²).

TC track/months	10-24-day OLR	30-60-day OLR
W-NW/MJ	-17.69	-6.10
W-NW/JAS	-10.47	-9.42
W-NW/ON	-10.05	-8.55
NE/MJ	-11.18	-12.14
N/JAS	-7.21	-7.15

reveals that 10-24-day OLR tends to be somewhat stronger or comparable in intensity than 30-60-day OLR in affecting SCS-formed TCs. However, 10-24-day OLR is not strong enough to dominate 30-60-day OLR in solely determining TC activity. In this case, the SCS-formed TCs are considered jointly modulated by both 10-24-day and 30-60-day ISOs with comparable importance.

8. MOISTURE FLUX ASSOCIATED WITH 30-60-DAY ISO

The above analyses have demonstrated that track variability of SCS-formed TCs follow closely the propagating of the 10-24-day ISO to take different tracks. The 30-60-day ISO moves slowly without evident propagation in concert with TC movement. However, its elongated cyclonic anomaly can provide favorable background environments

for TCs to move and develop. To delineate the favorable 30-60-day environments for TC movement, composite 30-60-day anomalies of moisture flux and divergence of moisture flux associated with different TC tracks are examined in this section. Moisture flux integrated from 1000 to 500 hPa is computed as $V_Q = \int_P^{P_0} Vq dp$, where V represents the horizontal wind vector, q is the specific humidity, P is 500 hPa, and P_0 is 1000 hPa. Divergence of moisture flux is computed as $\nabla \cdot V_Q$. Its negative patterns represent moisture convergence that is a favorable condition for TC development.

Composite 30-60-day anomalies of V_Q (vector) and $\nabla \cdot V_Q$ (shading) on the formation days of TCs for different track types are shown in Fig. 14. For TCs with W-NW tracks (Figs. 14a - c), 30-60-day V_Q anomalies exhibit elongated cyclonic moisture flux extending across the Bay of Bengal, SCS, and tropical WNP with a center overlying the SCS. The 30-60-day $\nabla \cdot V_Q$ anomalies show convergent (negative)
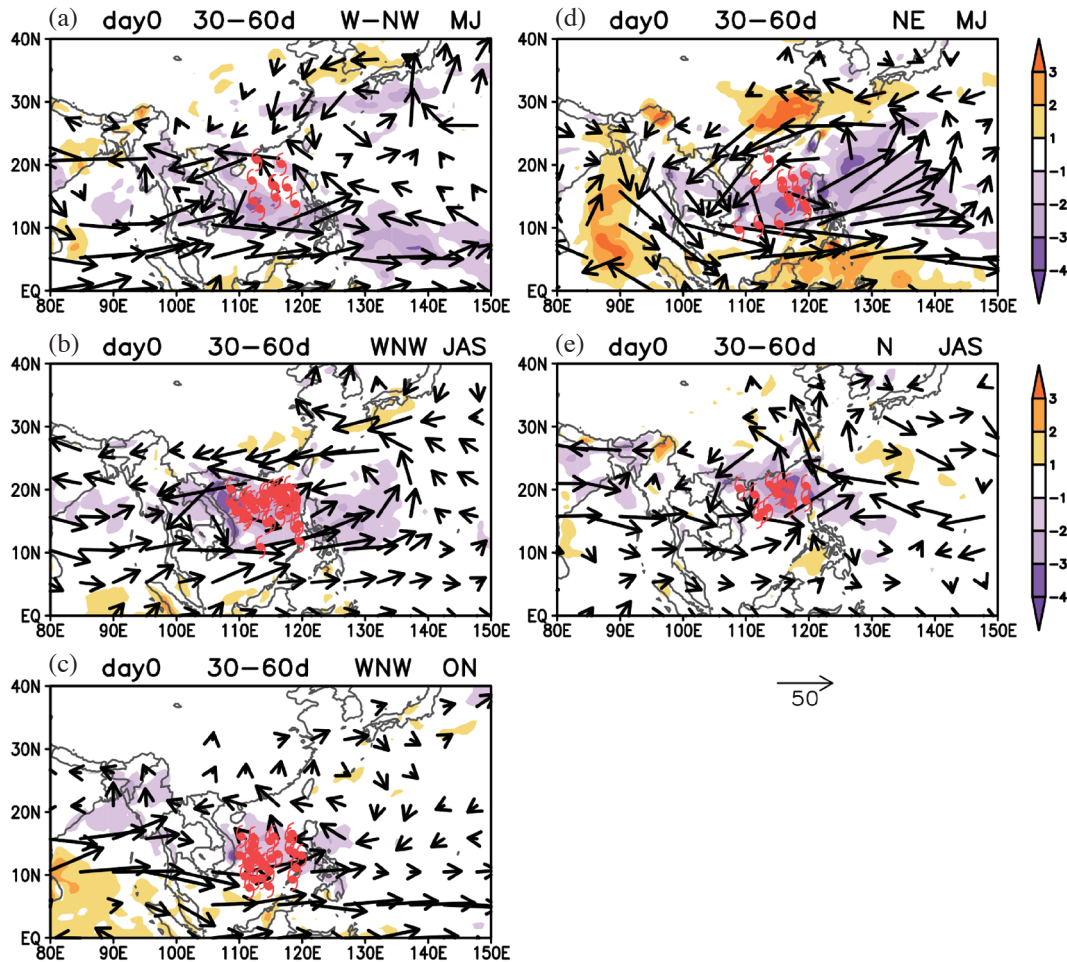
Fig. 14. Composite patterns of 30-60-day moisture flux (vector) and divergence of moisture flux (shading) on the formation day of TCs for different tracks in different seasonal periods: (a) W-NW tracks during May to June, (b) W-NW tracks during July to September, (c) W-NW tracks during October to November, (d) NE tracks during May to June, and (e) N tracks during July to September. TC locations on the formation day in each period are marked by TC symbols. Unit: g Kg^{-1} ms^{-1} for moisture flux and 10^{-5} g Kg^{-1} s^{-1} for divergence of moisture flux.

patterns along the cyclonic moisture flux to extend from the SCS westward and northwestward toward the Indochina Peninsula and the Bay of Bengal. This W-NW-extending moisture convergence anomaly gives favorable conditions assisting westward and northwestward movement for TC development. For TCs with NE (Fig. 14d) and N (Fig. 14e) tracks, negative $\nabla \cdot V_Q$ anomalies contain a regional center in the SCS to match TC formation. In addition, they stretch from the SCS northeastward across Taiwan and the Philippines to provide favorable conditions for TCs with NE tracks, while the extension becomes northward into southern China for TCs with N tracks. The above analyses illustrate that moisture convergence associated with a 30-60-day ISO modulates TC movement by providing favorable environments along TC tracks. TCs move in accordance with different spatial patterns of favorable 30-60-day environments resulting in different types of TC tracks.

9. CONCLUDING REMARKS

Tracks of TCs that form inside the SCS (referred to as SCS-formed TCs) have been examined, focusing on their seasonal variability and associated modulations by seasonal and intraseasonal circulations. The major tracks of SCS-formed TCs are separated into three types: northeastward (NE) toward the Philippines and Taiwan, northward (N) toward southern China, and westward-northwestward (W-NW) toward the Indochina Peninsula and southwestern China. Based on the 1979 - 2010 JTWC data, our analyses reveal a clear seasonal variability feature in tracks of SCS-formed TCs. The dominant track is NE in May and changes from NE into W-NW in June. The season of July to September has a prevailing W-NW track that is followed by a N track. In October and November, the primary track is W-NW in accordance with a southward displacement of the equatorial trough.

Formation of TCs with different tracks are associated with different circulation features. TCs with W-NW tracks tend to form within a cyclonic circulation overlying the SCS that is paired with a subtropical high on its northern side. Strong easterly flows between this cyclonic and anticyclonic circulation pair steer TCs forming inside the SCS to take W-NW tracks. TCs with NE tracks form inside a cyclonic shear with a strong subtropical high on the eastern side. The strong southwesterly flows between this circulation pair drive TCs from the SCS northward and later turn them eastward through subtropical westerly flows. TCs with N tracks are formed inside a cyclonic circulation over the SCS with a relatively lower-pressure region to the north. The formed TCs thus move northward toward the lower-pressure region over southern China. The WPSH and MT exhibit noticeable variability to modulate TC tracks on the formation day. In MJ, an eastward-intensified MT and a northwestward shifted WPSH guide TCs to take W-NW tracks, while an eastward-intensified MT and an eastward-retreating WPSH steer TCs to take NE tracks. In JAS, a southward-intensified MT and a strong westward-expanding WPSH result in W-NW tracks, while a northward-intensified MT and a northwestward-extending WPSH drive TCs to take N tracks. In ON, TCs with W-NW tracks match a westward and northward intensification of the equatorial trough.

ISO modulations of TC movements along different tracks show some common and discrepant features. In terms of common features, TCs in the SCS tend to form within the center of a 10-24-day cyclonic anomaly and follow its propagation to result in different tracks. Meanwhile, a 30-60-day cyclonic anomaly distributing along TC tracks provides a favorable environment with evident moisture convergence for the movement and development of TCs. The 30-60-day cyclonic anomaly also provides persistent steering flows to facilitate TC movement. Regarding different features, the 10-24-day cyclonic anomaly propagates in different directions guiding TCs along different tracks. A northwestward propagation of the 10-24-day cyclonic anomaly results in W-NW TC tracks. The 10-24-day cyclonic anomaly moves northward leading the northward movement of TCs. When it propagates northeastward, this is accompanied by NE tracks of TC movement. The 30-60-day cyclonic anomaly tends to exhibit a more elongated pattern across South Asia, the SCS, and the tropical WNP for TCs with W-NW tracks, but it exhibits a regional pattern for TCs with NE- or N tracks. The cyclonic anomaly is mainly over the SCS and WNP with a northeastward extension into the northwestern Pacific for TCs with NE tracks. It becomes only evident over the SCS and southern China for TCs with N tracks. These comparisons clearly indicate that the propagation of the 10-24-day ISO and spatial distributions of the 30-60-day ISO are two important factors in modulating movement of SCS-formed TCs. Convective anomalies associated with 10-24-day and 30-60-day ISOs exhibit comparable intensity to affect SCS-formed TCs. This indicates that activity of the SCS-formed TCs is jointly modulated by both 10-24-day and 30-60-day ISOs with comparable importance.

Our analysis shows that TC movement tends to closely follow the propagation of the 10-24-day cyclonic anomaly. This spatial relationship is probably related to the issue raised by Aiyyer et al. (2012) as the possible mixture of TC signals and the 10-24-day ISO due to their closeness in frequency bands and spatial scales. However, this issue needs to be comprehensively delineated by future studies. On the other hand, the 30-60-day ISO exhibits a much larger spatial pattern and a much longer frequency band than TCs. It is generally considered to be much less influenced by TC signals (Wu and Takahashi 2018). As such, its modulating effects on TC movement is considered to be independent of TC signals. The 30-60-day ISO provides a large-scale favorable environment for TCs to move in and develop. TC tracks are thus affected and modulated.

The above large-scale patterns on the formation day of TCs, including real-time patterns of steering flows, variability features of the MT and WPSH, and ISO anomaly patterns, can serve as key monitoring features to predict TC movement in different periods of the active TC season. These identified features may provide guidance to improve forecasts of TC movement in the SCS.

REFERENCES

Aiyyer, A., A. Mekonnen, and C. J. Schreck, 2012: Projection of tropical cyclones on wavenumber-frequency-filtered equatorial waves. *J. Clim.*, **25**, 3653-3658, doi: 10.1175/JCLI-D-11-00451.1. [Link]

Barrett, B. S. and L. M. Leslie, 2009: Links between tropical cyclone activity and Madden-Julian oscillation phase in the North Atlantic and Northeast Pacific basins. *Mon. Weather Rev.*, **137**, 727-744, doi: 10.1175/2008MWR2602.1. [Link]

Bell, R., K. Hodges, P. L. Vidale, J. Strachan, and M. Roberts, 2014: Simulation of the global ENSO-tropical cyclone teleconnection by a high-resolution coupled general circulation model. *J. Clim.*, **27**, 6404-6422, doi: 10.1175/JCLI-D-13-00559.1. [Link]

Camargo, S. J., A. W. Robertson, S. J. Gaffney, P. Smyth, and M. Ghil, 2007: Cluster analysis of typhoon tracks. Part I: General properties. *J. Clim.*, **20**, 3635-3653, doi: 10.1175/JCLI4188.1. [Link]

Chan, J. C. L., 2000: Tropical cyclone activity over the western North Pacific associated with El Niño and La Niña events. *J. Clim.*, **13**, 2960-2972, doi: 10.1175/1520-0442(2000)013<2960:TCAOTW>2.0.CO;2. [Link]

Chand, S. S. and K. J. E. Walsh, 2010: The Influence of the Madden-Julian oscillation on tropical cyclone activity in the Fiji region. *J. Clim.*, **23**, 868-886, doi: 10.1175/2009JCLI3316.1. [Link]

Chen, G., 2011: How does shifting Pacific Ocean warming modulate on tropical cyclone frequency over the South China Sea? *J. Clim.*, **24**, 4695-4700, doi: 10.1175/2011JCLI4140.1. [Link]

Chen, J.-M., P.-H. Tan, L. Wu, J.-S. Liu, and H.-S. Chen, 2017: Climatological analysis of passage-type tropical cyclones from the western North Pacific into the South China Sea. *Terr. Atmos. Ocean. Sci.*, **28**, 327-343, doi: 10.3319/TAO.2016.10.04.02. [Link]

Chen, J.-M., P.-H. Tan, L. Wu, H.-S. Chen, J.-S. Liu, and C.-F. Shih, 2018a: Interannual variability of summer tropical cyclone rainfall in the western North Pacific depicted by CFSR and associated large-scale processes and ISO modulations. *J. Clim.*, **31**, 1771-1787, doi: 10.1175/JCLI-D-16-0805.1. [Link]

Chen, J.-M., C.-H. Wu, P.-H. Chung, and C.-H. Sui, 2018b: Influence of intraseasonal-interannual oscillations on tropical cyclone genesis in the Western North Pacific. *J. Clim.*, **31**, 4949-4961, doi: 10.1175/JCLI-D-17-0601.1. [Link]

Chen, J.-M., C.-H. Wu, J. Gao, P.-H. Chung, and C.-H. Sui, 2019: Migratory tropical cyclones in the South China Sea modulated by intraseasonal oscillations and climatological circulations. *J. Clim.*, **32**, 6445-6466, doi: 10.1175/JCLI-D-18-0824.1. [Link]

Chen, T.-C. and J.-M. Chen, 1995: An observational study of the South China Sea monsoon during the 1979 summer: Onset and life cycle. *Mon. Weather Rev.*, **123**, 2295-2318, doi: 10.1175/1520-0493(1995)123<2295:AOSOTS>2.0.CO;2. [Link]

Chen, T.-C., S.-P. Weng, N. Yamazaki, and S. Kiehne, 1998: Interannual variation in the tropical cyclone formation over the western North Pacific. *Mon. Weather Rev.*, **126**, 1080-1090, doi: 10.1175/1520-0493(1998)126<1080:IVITTC>2.0.CO;2. [Link]

Chen, T.-C., M.-C. Yen, and S.-P. Weng, 2000: Interaction between the summer monsoons in East Asia and the South China Sea: Intraseasonal monsoon modes. *J. Atmos. Sci.*, **57**, 1373-1392, doi: 10.1175/1520-0469(2000)057<1373:IBTSMI>2.0.CO;2. [Link]

Chen, T.-C., S.-Y. Wang, M.-C. Yen, and A. J. Clark, 2009: Impact of the intraseasonal variability of the western North Pacific large-scale circulation on tropical cyclone tracks. *Weather Forecast.*, **24**, 646-666, doi: 10.1175/2008WAF2222186.1. [Link]

Chia, H. H. and C. F. Ropelewski, 2002: The interannual variability in the genesis location of tropical cyclones in the northwest Pacific. *J. Clim.*, **15**, 2934-2944, doi: 10.1175/1520-0442(2002)015<2934:TIVITG>2.0.CO;2. [Link]

Chung, P.-H. and T. Li, 2015: Characteristics of tropical cyclone genesis in the western North Pacific during the developing and decaying phases of two types of El Niño. *Journal of Tropical Meteorology*, **21**, 14-22.

Colbert, A. J., B. J. Soden, and B. P. Kirtman, 2015: The Impact of Natural and Anthropogenic Climate Change on Western North Pacific Tropical Cyclone Tracks. *J. Clim.*, **28**, 1806-1823, doi: 10.1175/JCLI-D-14-00100.1. [Link]

Corporal-Lodangco, I. L., L. M. Leslie, and P. J. Lamb, 2016: Impacts of ENSO on Philippine tropical cyclone activity. *J. Clim.*, **29**, 1877-1897, doi: 10.1175/JCLI-D-14-00723.1. [Link]

Dee, D. P., S. M. Uppala, A. J. Simmons, P. Berrisford, P. Poli, S. Kobayashi, U. Andrae, M. A. Balmaseda, G. Balsamo, P. Bauer, P. Bechtold, A. C. M. Beljaars, L. van de Berg, J. Bidlot, N. Bormann, C. Delsol, R. Dragani, M. Fuentes, A. J. Geer, L. Haimberger, S. B. Healy, H. Hersbach, E. V. Hólm, L. Isaksen, P. Kåll- berg, M. Köhler, M. Matricardi, A. P. McNally, B. M. Monge-Sanz, J.-J. Morcrette, B.-K. Park, C. Peubey, P. de Rosnay, C. Tavolato, J.-N. Thépaut, and F. Vi- tart, 2011: The ERA-interim reanalysis: Configuration and performance of the data assimilation system. *Q. J. R. Meteorol. Soc.*, **137**, 553-597, doi: 10.1002/qj.828. [Link]

Ding, Y., 1994: Monsoons over China, Springer Nether- lands, 420 pp, doi: 10.1007/978-94-015-8302-2. [Link]

Ding, Y., 2007: The variability of the Asian summer mon- soon. *J. Meteorol. Soc. Jpn.*, **85B**, 21-54, doi: 10.2151/ jmsj.85B.21. [Link]

Duchon, C. E., 1979: Lanczos filtering in one and two di- mensions. *J. Appl. Meteorol.*, **18**, 1016-1022, doi: 10.1175/1520-0450(1979)018<1016:LFIOAT>2.0. CO;2. [Link]

Hall, J. D., A. J. Matthews, and D. J. Karoly, 2001: The modulation of tropical cyclone activity in the Australian region by the Madden-Julian oscilla- tion. *Mon. Weather Rev.*, **129**, 2970-2982, doi: 10.1175/1520-0493(2001)129<2970:TMOTCA>2.0. CO;2. [Link]

Harr, P. A. and R. L. Elsberry, 1991: Tropical cyclone track characteristics as a function of large-scale circulation anomalies. *Mon. Weather Rev.*, **119**, 1448-1468, doi: 10.1175/1520-0493(1991)119<1448:TCTCAA>2.0. CO;2. [Link]

Hartmann, D. L., M. L. Michelsen, and S. A. Klein, 1992: Seasonal variations of tropical intraseasonal oscillations: A 20-25-day oscillation in the west- ern Pacific. *J. Atmos. Sci.*, **49**, 1277-1289, doi: 10.1175/1520-0469(1992)049<1277:SVOTIO>2.0. CO;2. [Link]

Huang, P., C. Chou, and R. Huang, 2011: Seasonal modu- lation of tropical intraseasonal oscillations on tropical cyclone geneses in the western North Pacific. *J. Clim.*, **24**, 6339-6352, doi: 10.1175/2011JCLI4200.1. [Link]

Kim, H.-M., M.-I. Lee, P. J. Webster, D. Kim, and J. H. Yoo, 2013: A physical basis for the probabilistic prediction of the accumulated tropical cyclone kinetic energy in the western North Pacific. *J. Clim.*, **26**, 7981-7991, doi: 10.1175/JCLI-D-12-00679.1. [Link]

Kim, J.-H., C.-H. Ho, H.-S. Kim, and W. Choi, 2012: 2010 Western North Pacific Typhoon Season: Seasonal Overview and Forecast Using a Track-Pattern-Based Model. *Weather Forecast.*, **27**, 730-743, doi: 10.1175/ WAF-D-11-00109.1. [Link]

Klein, S. A., B. J. Soden, and N.-C. Lau, 1999: Remote sea surface temperature variations during ENSO: Evidence for a tropical atmospheric bridge. *J. Clim.*, **12**, 917- 932, doi: 10.1175/1520-0442(1999)012<0917:RSSTV D>2.0.CO;2. [Link]

Klotzbach, P. J., 2014: The Madden-Julian Oscillation's im- pacts on worldwide tropical cyclone activity. *J. Clim.*, **27**, 2317-2330, doi: 10.1175/JCLI-D-13-00483.1. [Link]

Ko, K.-C. and H.-H. Hsu, 2009: ISO modulation on the sub- monthly wave pattern and recurving tropical cyclones in the tropical western North Pacific. *J. Clim.*, **22**, 582- 599, doi: 10.1175/2008JCLI2282.1. [Link]

Kubota, H. and J. C. L. Chan, 2009: Interdecadal variabil- ity of tropical cyclone landfall in the Philippines from 1902 to 2005. *Geophys. Res. Lett.*, **36**, L12802, doi: 10.1029/2009GL038108. [Link]

Lander, M. A., 1994: An exploratory analysis of the rela- tionship between tropical storm formation in the west- ern North Pacific and ENSO. *Mon. Weather Rev.*, **122**, 636-651, doi: 10.1175/1520-0493(1994)122<0636:AE AOTR>2.0.CO;2. [Link]

Lander, M. A., 1996: Specific tropical cyclone track types and unusual tropical cyclone motions associated with a reverse-oriented monsoon trough in the western North Pacific. *Weather Forecast.*, **11**, 170-186, doi: 10.1175/1520-0434(1996)011<0170:STCTTA>2.0. CO;2. [Link]

Lau, N.-C. and M. J. Nath, 2000: Impact of ENSO on the variability of the Asian-Australian monsoons as simu- lated in GCM experiments. *J. Clim.*, **13**, 4287-4309, doi: 10.1175/1520-0442(2000)013<4287:IOEOTV>2. 0.CO;2. [Link]

Lau, N.-C. and M. J. Nath, 2003: Atmosphere- ocean variations in the Indo-Pacific sector dur- ing ENSO episodes. *J. Clim.*, **16**, 3-20, doi: 10.1175/1520-0442(2003)016<0003:AOVITI>2.0. CO;2. [Link]

Li, R. C. Y. and W. Zhou, 2013: Modulation of western North Pacific tropical cyclone activity by the ISO. Part II: Tracks and landfalls. *J. Clim.*, **26**, 2919-2930, doi: 10.1175/JCLI-D-12-00211.1. [Link]

Liebmann, B. and C. A. Smith, 1996: Description of a com- plete (interpolated) outgoing longwave radiation data- set. *Bull. Amer. Meteorol. Soc.*, **77**, 1275-1277. Avail- able at https://www.jstor.org/stable/26233278.

Liebmann, B., H. H. Hendon, and J. D. Glick, 1994: The re- lationship between tropical cyclones of the western Pa- cific and Indian Oceans and the Madden-Julian oscilla- tion. *J. Meteorol. Soc. Jpn.*, **72**, 401-411, doi: 10.2151/ jmsj1965.72.3_401. [Link]

Lin, Y.-L. and C.-S. Lee, 2011: An analysis of tropical cy- clone formations in the South China Sea during the late season. *Mon. Weather Rev.*, **139**, 2748-2760, doi: 10.1175/2011MWR3495.1. [Link]

Ling, Z., Y. Wang, and G. Wang, 2016: Impact of intraseasonal oscillations on the activity of tropical cyclones in summer over the South China Sea. Part I: Local tropical cyclones. *J. Clim*., **29**, 855-868, doi: 10.1175/JCLI-D-15-0617.1. [Link]

Mao, J. and J. C. L. Chan, 2005: Intraseasonal variability of the South China Sea summer monsoon. *J. Clim*., **18**, 2388-2402, doi: 10.1175/JCLI3395.1. [Link]

Nakazawa, T. and K. Rajendran, 2007: Relationship between tropospheric circulation over the western North Pacific and tropical cyclone approach/landfall on Japan. *J. Meteorol. Soc. Jpn*., **85**, 101-114, doi: 10.2151/jmsj.85.101. [Link]

Su, O.-H. and F. Xue, 2011: Two northward jumps of the summertime western Pacific subtropical high and their associations with the tropical SST anomalies. *Atmos. Ocean. Sci. Lett*., **4**, 98-102, doi: 10.1080/16742834.2011.11446910. [Link]

Tan, P.-H., J.-Y. Tu, L. Wu, H.-S. Chen, and J.-M. Chen, 2019: Asymmetric relationships between El Niño-Southern Oscillation and entrance tropical cyclones in the South China Sea during fall. *Int. J. Climatol*., **39**, 1872-1888, doi: 10.1002/joc.5921. [Link]

Tu, J.-Y. and J.-M. Chen, 2019: Large-scale indices for assessing typhoon activity around Taiwan. *Int. J. Climatol*., **39**, 921-933, doi: 10.1002/joc.5852. [Link]

Wang, B., 1992: The vertical structure and development of the ENSO anomaly mode during 1979-1989. *J. Atmos. Sci*., **49**, 698-712, doi: 10.1175/1520-0469(1992)049<0698:TVSADO>2.0.CO;2. [Link]

Wang, B. and J. C. L. Chan, 2002: How strong ENSO events affect tropical storm activity over the western North Pacific. *J. Clim*., **15**, 1643-1658, doi: 10.1175/1520-0442(2002)015<1643:HSEEAT>2.0.CO;2. [Link]

Wang, G., J. Su, Y. Ding, and D. Chen, 2007: Tropical cyclone genesis over the south China sea. *J. Mar. Syst*., **68**, 318-326, doi: 10.1016/j.jmarsys.2006.12.002. [Link]

Wu, L. and M. Takahashi, 2018: Contributions of tropical waves to tropical cyclone genesis over the western North Pacific. *Climate Dyn*., **50**, 4635-4649, doi: 10.1007/s00382-017-3895-3. [Link]

Wu, L., Z. Wen, R. Huang, and R. Wu, 2012: Possible Linkage between the Monsoon Trough Variability and the Tropical Cyclone Activity over the Western North Pacific. *Mon. Weather Rev*., **140**, 140-150, doi: 10.1175/MWR-D-11-00078.1. [Link]

Wu, R., 2002: Processes for the northeastward advance of the summer monsoon over the western North Pacific. *J. Meteorol. Soc. Jpn*., **80**, 67-83, doi: 10.2151/jmsj.80.67. [Link]

Yang, L., Y. Du, D. Wang, C. Wang, and X. Wang, 2015: Impact of intraseasonal oscillation on the tropical cyclone track in the South China Sea. *Climate Dyn*., **44**, 1505-1519, doi: 10.1007/s00382-014-2180-y. [Link]

Zhan, R., Y. Wang, and X. Lei, 2011: Contributions of ENSO and east Indian Ocean SSTA to the interannual variability of Northwest Pacific tropical cyclone frequency. *J. Clim*., **24**, 509-521, doi: 10.1175/2010JCLI3808.1. [Link]